

Mechanism of Particulate Matter-associated Respiratory Inflammation

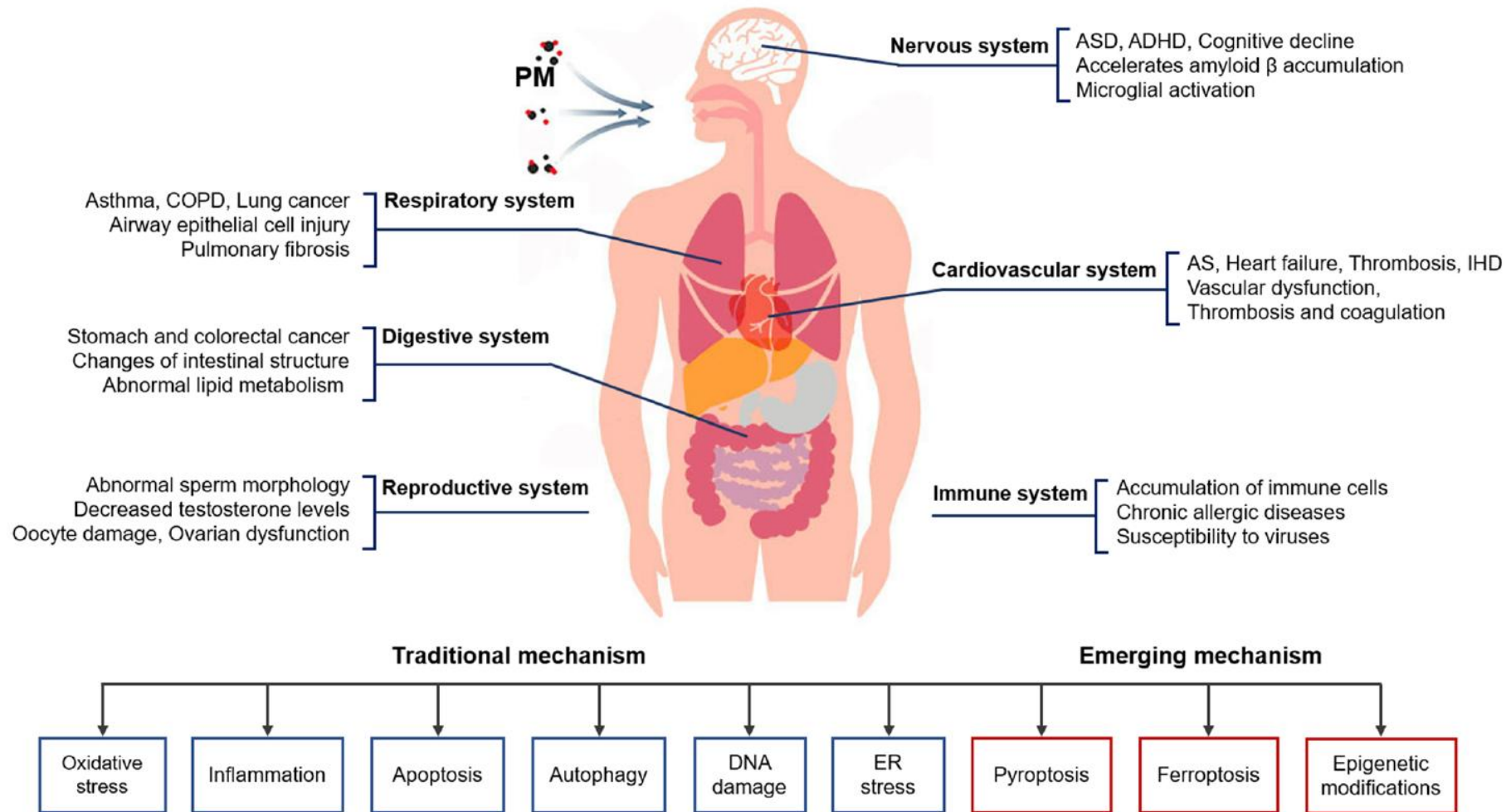
March 21, 2026

Gachon University Gil Medical Center

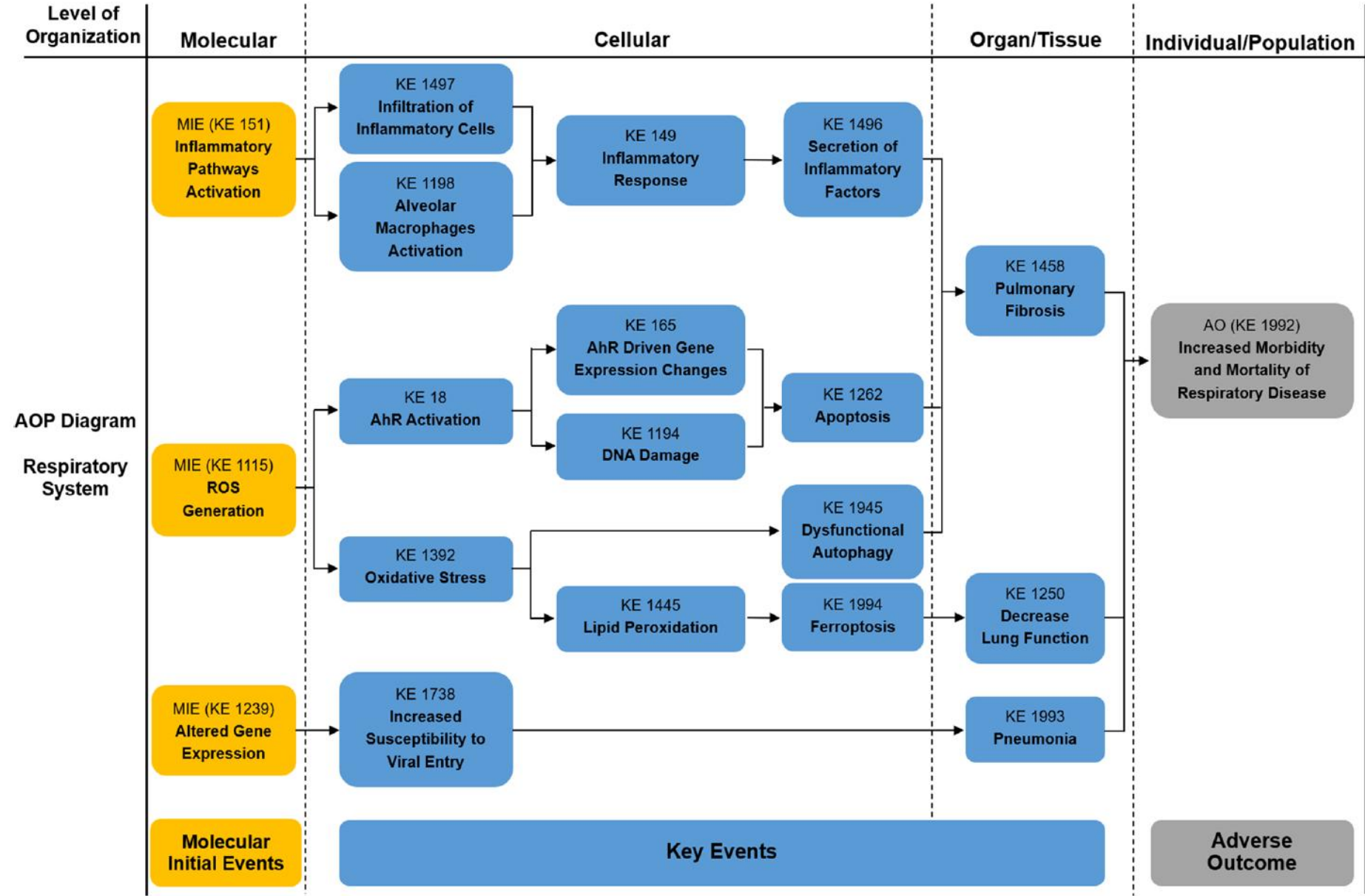
Sun Young Kyung

Ambient PM on the adverse health effects based from laboratory evidence

Li T et al. Particle and Fibre Toxicology 2022

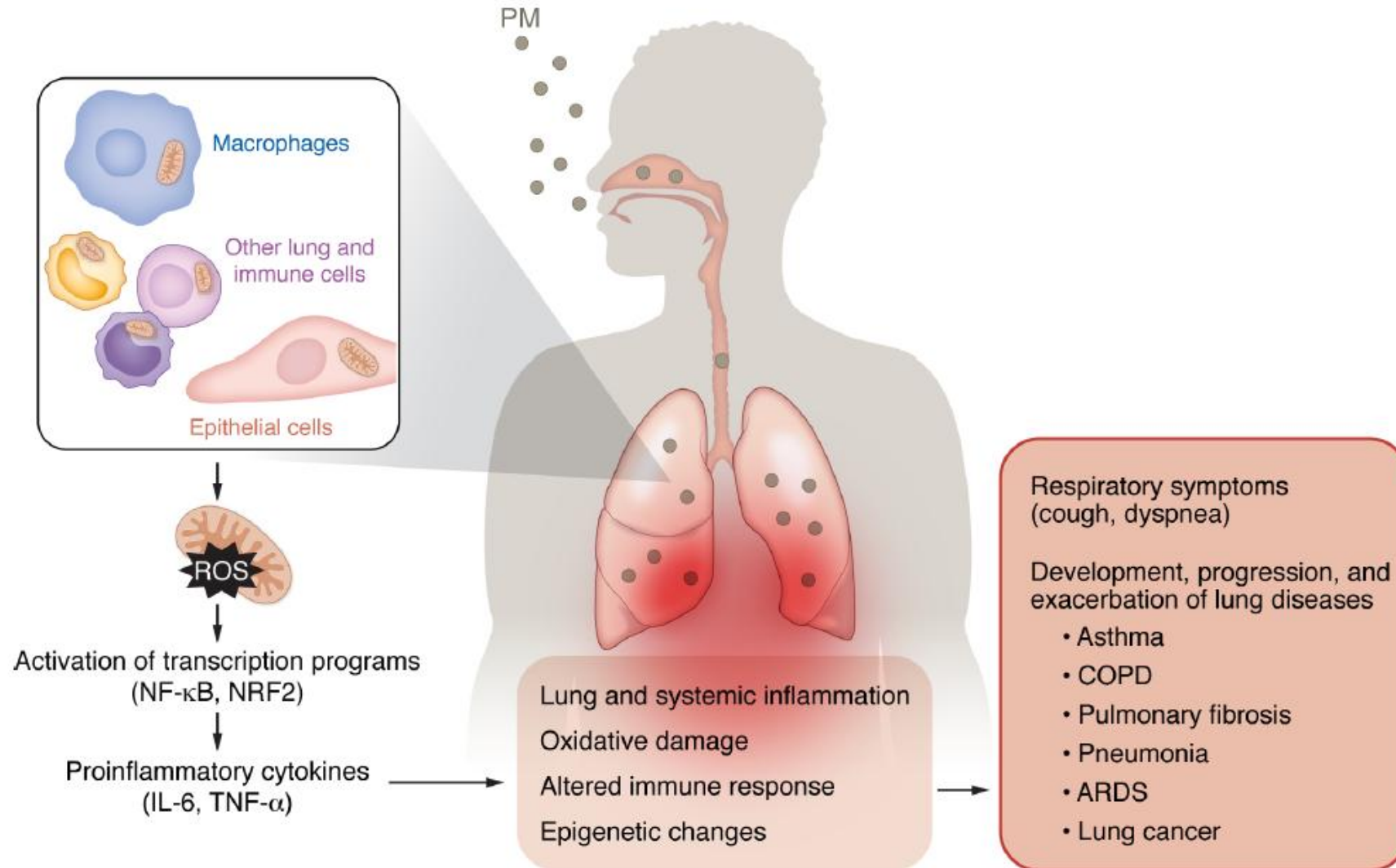


Adverse outcome pathways diagram related to PM associated respiratory toxicity



Mechanisms by which PM air pollution affects the respiratory system

Robert B et al. J Clin Invest 2025



Oxidative Stress and Inflammation

- ✓ PM metals and organic compounds generate reactive oxygen species (ROS) and inflammation in lung cells.

Smith KR et al. Chem Res Toxicol 1997
Kumagai Y et al. Free Radic Biol Med 1997

- ✓ PM exposure induces pro-inflammatory cytokine production (IL-1 β , IL-6, IL-8, TNF- α).

Becker S et al. Toxicol Appl Pharmacol 2005

- ✓ PM activates MAPK and NF- κ B signaling.

Takizawa H et al. J Immunol 1999

- ✓ Ultrafine particulate pollutants induce mitochondrial damage.

Li N et al. Environ Health Perspect 2003

Ultrafine Particulate Pollutants Induce Oxidative Stress and Mitochondrial Damage

Li N et al. Environ Health Perspect 2003

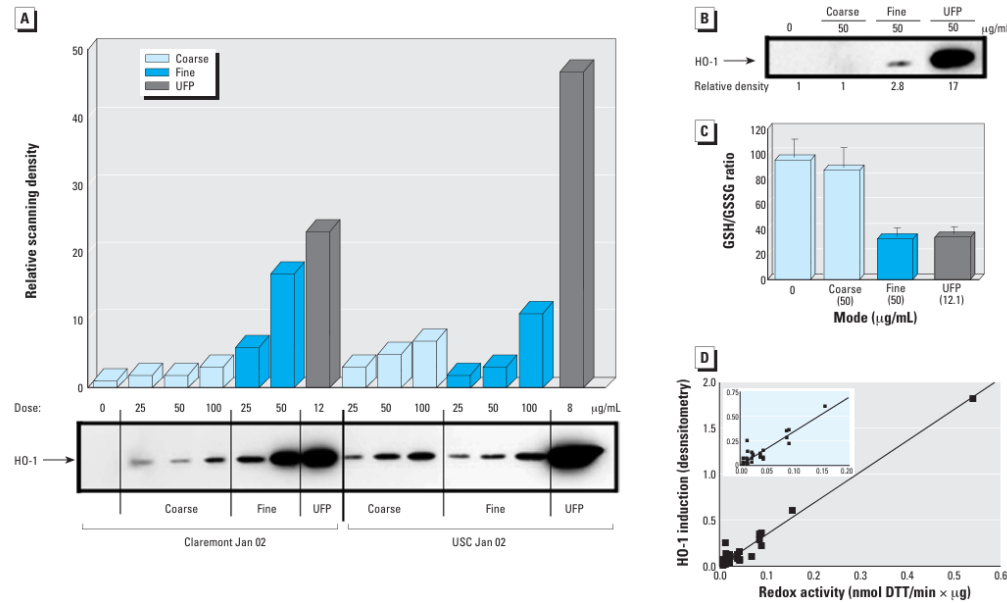


Figure 2. Induction of oxidative stress and HO-1 expression. (A) HO-1 expression in RAW 264.7 cells exposed to CAPs for 16 hr. (B) HO-1 expression in BEAS-2B cells treated with CAPs (Claremont Mar 02) for 16 hr. (C) Effects of CAPs (Claremont Jan 02) on the intracellular GSH/GSSG ratio in RAW 264.7 cells after 16 hr exposure; GSH/GSSG values shown are mean ± SEM from two separate experiments, with duplicate measurements per experiment (Tietze 1969). (D) Regression analysis demonstrating the correlation between *in vitro* redox activity of CAPs and HO-1 induction (15 data points); $r^2 = 0.97$. Inset: After removal of the highest data point, $r^2 = 0.81$.

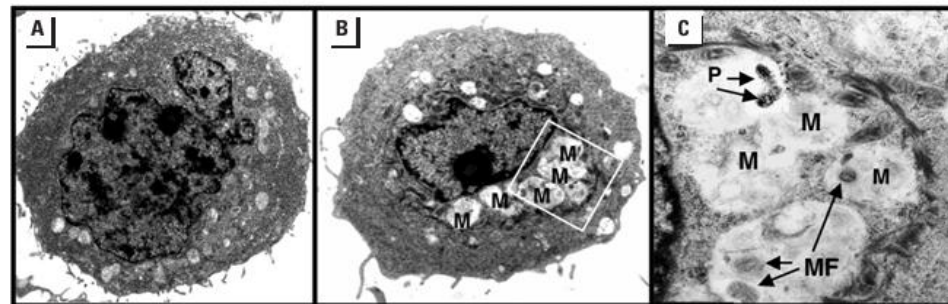


Figure 4. Electron micrographs demonstrating mitochondrial destruction in BEAS-2B cells treated with 8.4 µg/mL of USC-Jan 02 UFPs for 16 hr. (A) Untreated BEAS-2 cells; magnification ×8,500. (B) UFP-treated cells; magnification ×8,500. (C) UFP-treated cells; magnification ×26,300. Notice the disappearance of cristae, formation of myelin figures (MF), and presence of particles (P) inside mitochondria (M).

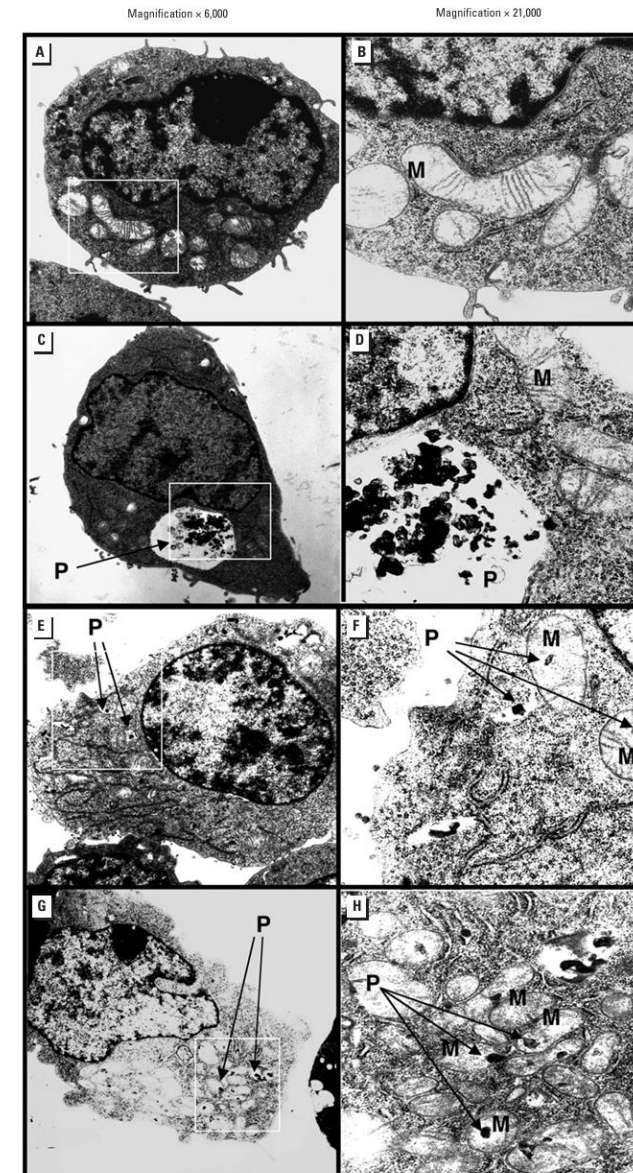
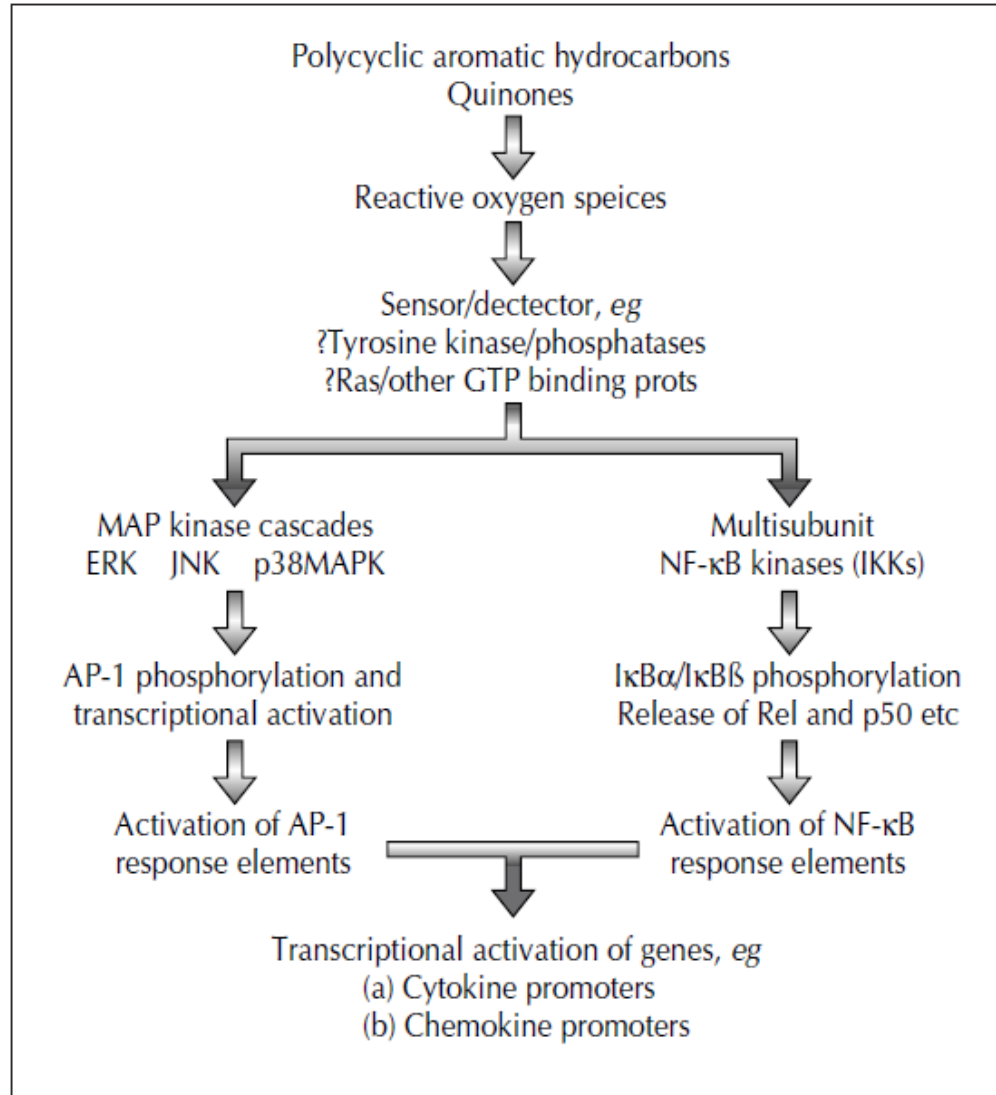


Figure 3. Electron micrographs demonstrating different sized particles in RAW 264.7 cells treated with USC-Jan 02 CAPs for 16 hr. (A) and (B) Untreated RAW 264.7 cells. (C) and (D) RAW 264.7 cells exposed to coarse particles. (E) and (F) RAW 264.7 cells exposed to fine particles. (G) and (H) RAW 264.7 cells exposed to UFPs. Notice damage to cristae as well as the presence of particles (P) inside mitochondria (M) in UFP- or fine + UFP-exposed cells.

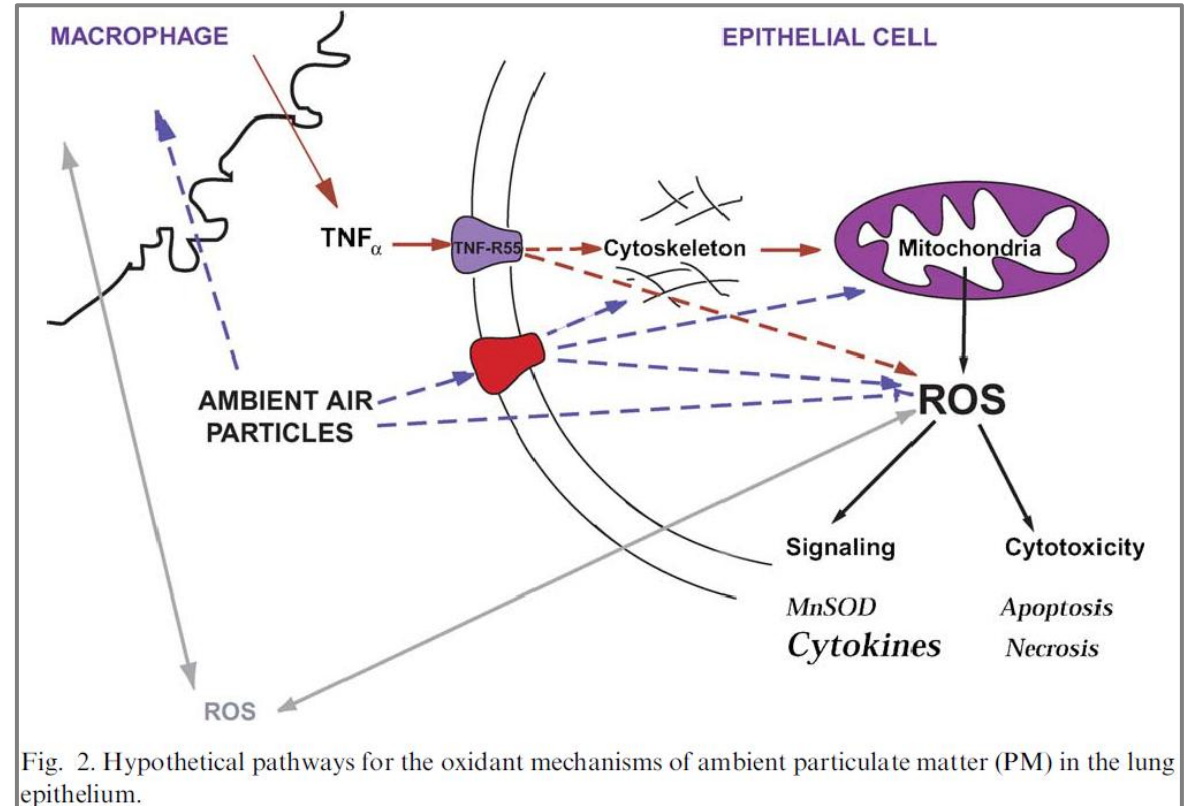
Figure 5. Activation of activator protein-1 (AP-1) and nuclear factor- κ B (NF- κ B) signaling pathways by reactive oxygen species (ROS)



Activation of AP-1 and NF- κ B signaling pathways by ROS plays a role in chemical-induced cytokine and chemokine expression.

Nel AE et al. Curr Opin Pulm Med 2001 [Review]

Oxidant mechanisms of ambient PM



Gonzalez-Flecha B et al. Mol Aspects Med 2004 [Review]

Epithelial Barrier Dysfunction

- ✓ DEP causes a reduction in epithelial barrier integrity through a reduction in the tight junction protein Tricellulin in the lungs.
- ✓ DEP reduced TEER, induced junction disruption and impaired mucociliary clearance in Air-liquid interface(ALI) airway models.

Smyth T et al. Particle Fibre Toxicol 2020

Diesel exhaust particle exposure reduces expression of the epithelial tight junction protein Tricellulin

Smyth T et al. Particle and Fibre Toxicology 2020

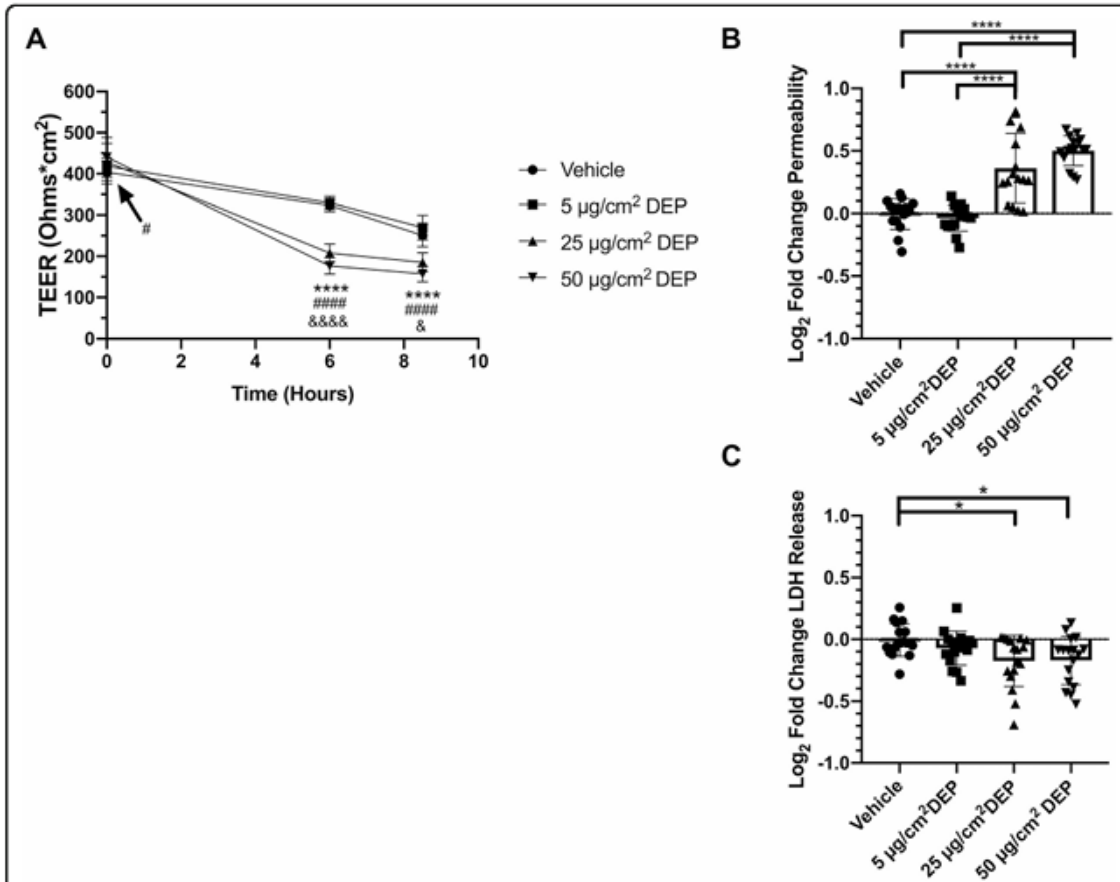
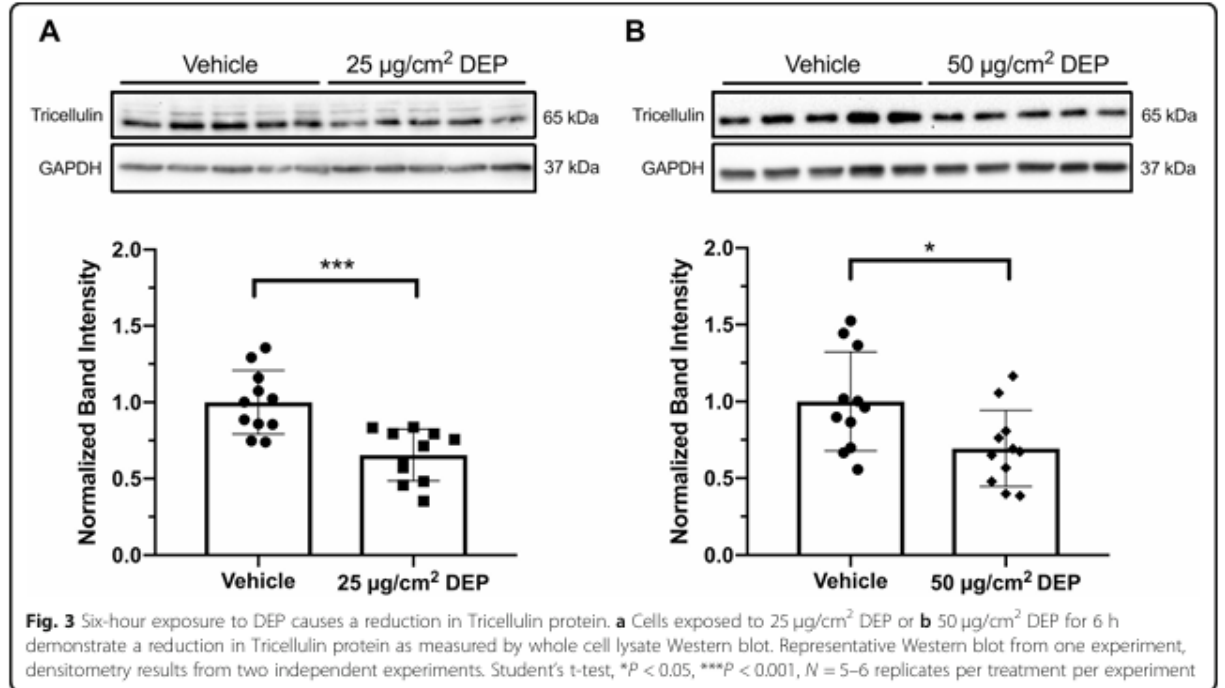
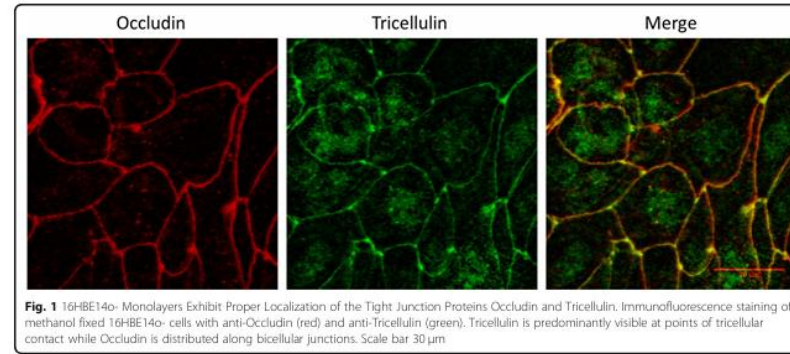
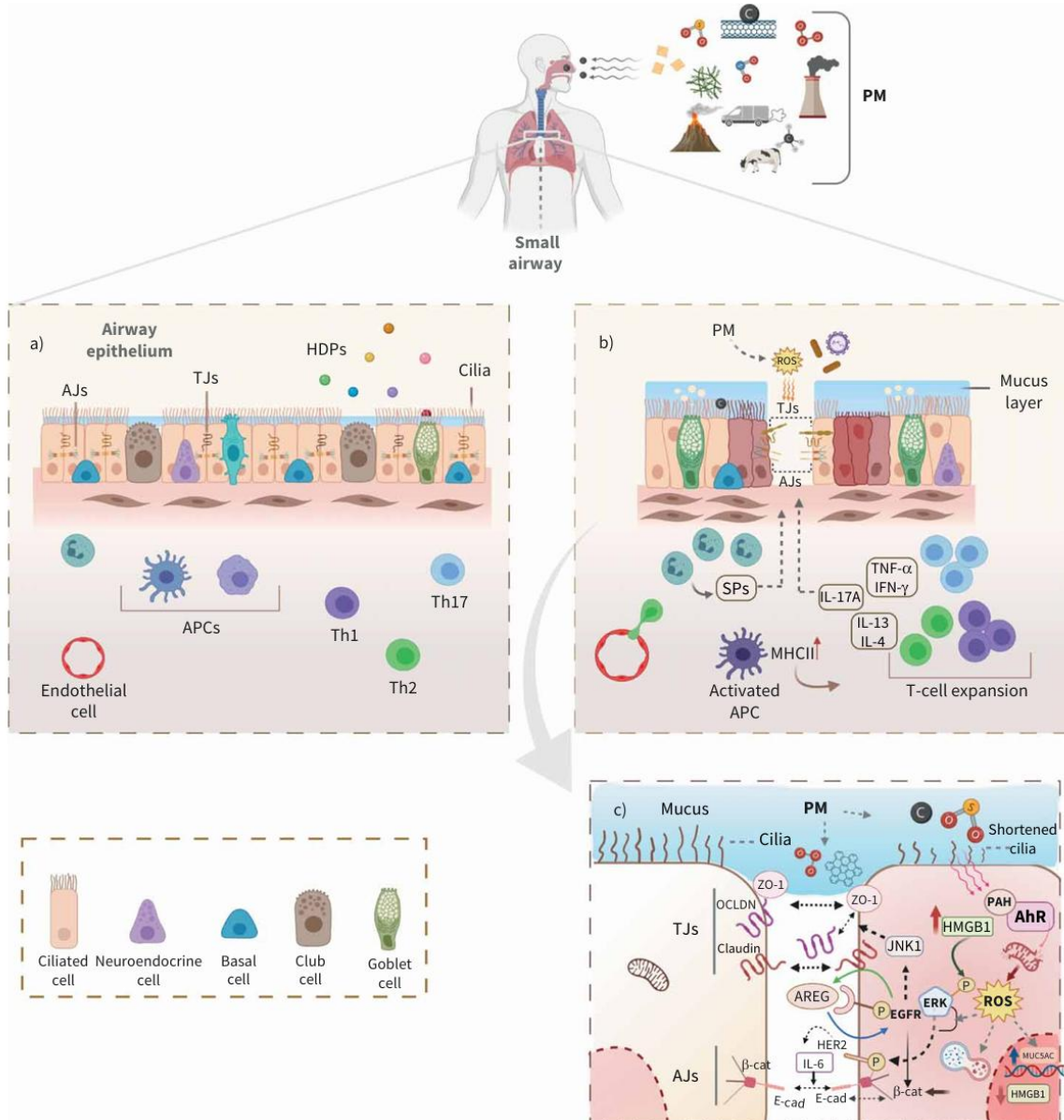


Fig. 2 Short term exposure to DEP reduces epithelial barrier function without causing cytotoxicity. **a** TEER measurements of cells exposed to indicated concentrations of DEP at time 0, 6, and 8.5 h after application of DEP. One-Way ANOVA with Tukey's HSD, **** $P < 0.0001$ Vehicle vs 25 µg/cm² DEP, # $P < 0.05$, #### $P < 0.0001$ Vehicle vs 50 µg/cm² DEP, & $P < 0.05$, &&&& $P < 0.0001$ 25 µg/cm² DEP vs 50 µg/cm² DEP. Data from three independent experiments, $N = 5-6$ replicates per treatment per time point per experiment. **b** 4 kDa FITC-Dextran permeability measured at 8.5 h after application of DEP. One-Way ANOVA with Tukey's HSD, **** $P < 0.0001$. Data from three independent experiments, $N = 5-6$ replicates per treatment per experiment. **c** Fold change LDH release normalized to average Vehicle LDH release. One-Way ANOVA, * $P < 0.05$. Data from three independent experiments, $N = 5-6$ replicates per treatment per time point per experiment



Epithelial Barrier Dysfunction



- ✓ AhR-mediated increase in ROS by mitochondria
- ✓ EGFR & ERK or ROS-mediated increased in HMGB1
- ✓ ROS-mediated increase in autophagy in AECs
- ✓ AREG or ROS \rightarrow EGFR activation \rightarrow AJs disruption, TJs permeability increase
- ✓ ERK activation \rightarrow HER2-mediated IL-6 increase \rightarrow trigger barrier dysfunction



Airway inflammation and remodeling: COPD, Asthma

FIGURE 1 Inhalation of air pollutants promotes airway epithelial barrier dysfunction. **a)** Healthy airway epithelium is protected against pathogens by physical junctions between the adjacent cells and by releasing innate immune HDPs. **b)** By exposure to airborne PM, the TJs and AJs between the AECs, including ZO-1, occludin and E-cadherin, are disrupted. Furthermore, PM induces mucociliary dysfunction by reducing cilia number, loss of cilia as well as goblet cell metaplasia leading to increased mucus production. PM entering the airway submucosa is presented to adaptive immune cells by APCs. PM-induced increase in MHCII on APCs leads to expansion of adaptive immune cells and production of inflammatory cytokines that further inflict airway epithelial barrier dysfunction. PM exposure also induces submucosal accumulation of neutrophils which may lead to barrier dysfunction by secretion of SPs. **c)** PM-induced barrier dysfunction is in part triggered by AhR-mediated increase in ROS generation by mitochondria and subsequent activation of EGFR and ERK or ROS-mediated increase in cytoplasmic HMGB1 and ROS-mediated increase in autophagy in AECs. Activation of EGFR either by PM-induced increase in AREG or ROS leads to disassembly in AJs by disrupting E-cadherin/ β -catenin, and increased TJs permeability by Rac1/JNK-mediated disruption in ZO-1 and occludin. Activation of ERK in turn triggers airway barrier dysfunction through HER2-mediated increase in IL-6. AEC: airway epithelial cell; AhR: aryl hydrocarbon receptor; AJ: adherens junction; APC: antigen-presenting cell; AREG: amphiregulin; β -cat: β -catenin; E-cad: E-cadherin; EGFR: epidermal growth factor receptor; ERK: extracellular signal-regulated kinase; HDP: host defence proteins and peptide; HER2: human epidermal receptor 2; HMGB1: high-mobility group box 1; IFN: interferon; IL: interleukin; JNK: c-jun N-terminal kinase; MHCII: major histocompatibility complex class II; MUC5AC: mucin 5AC; OCLDN: occludin; PAH: polyaromatic hydrocarbon; PM: particulate matter; ROS: reactive oxygen species; SP: serine protease; Th: T-helper cell; TJ: tight junction; TNF: tumour necrosis factor; ZO-1: zonula occludens-1. Figure partially created with BioRender.com.

Air-Liquid Interface (ALI) Airway Models

- ✓ Primary human airway epithelial cells
- ✓ Differentiation into ciliated, club, goblet cells
- ✓ Widely used to study PM epithelial responses

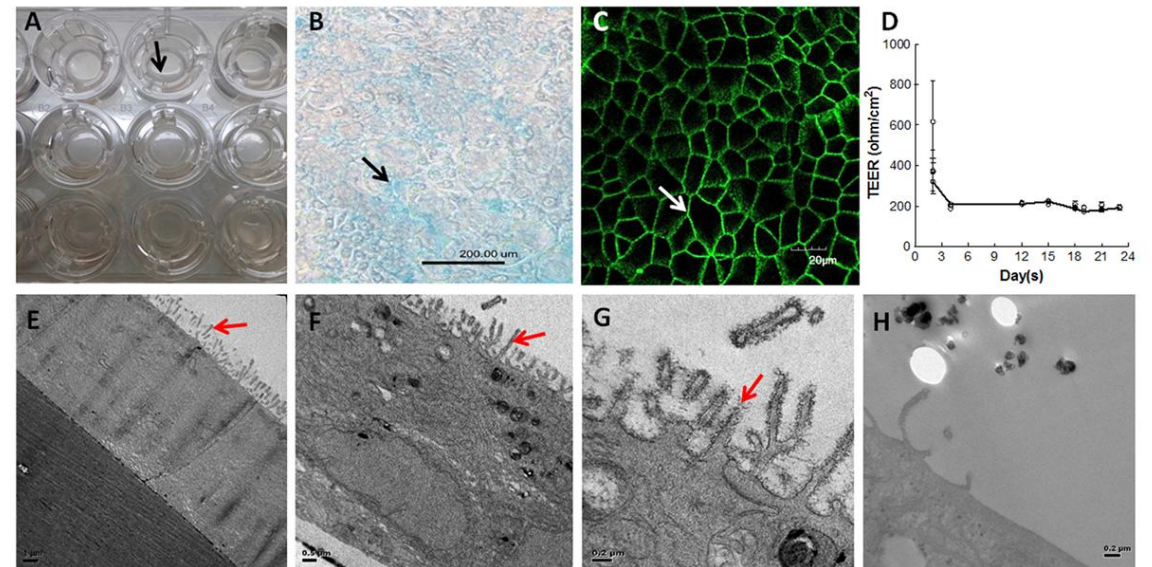
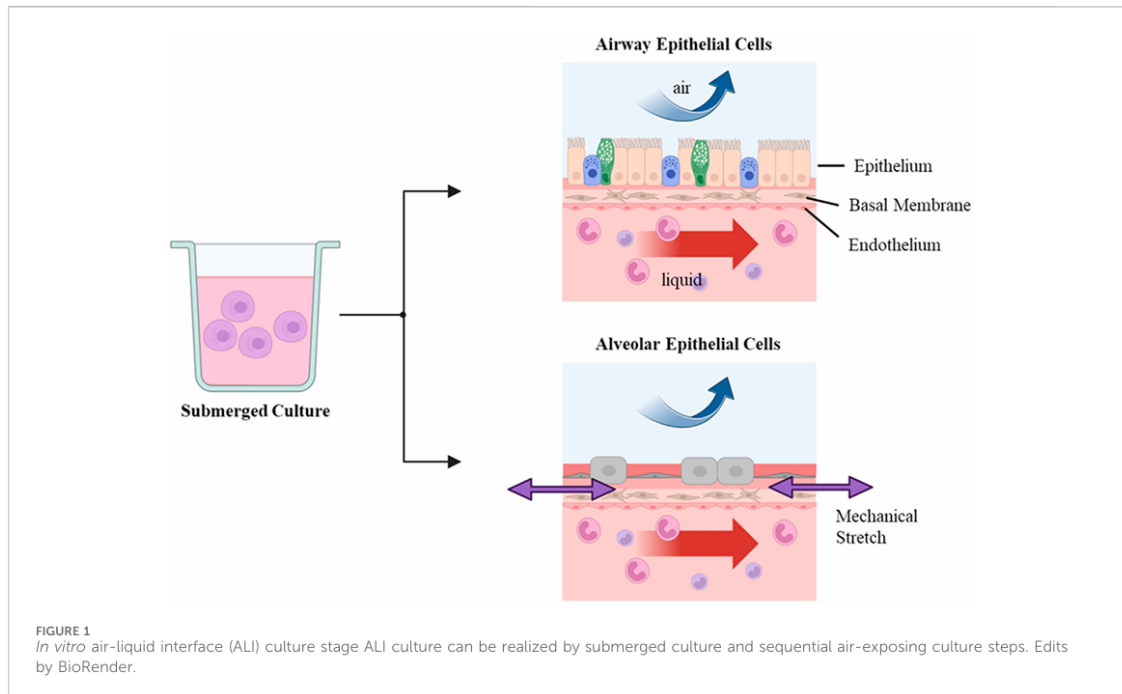


Fig. 1. Characterization of S-ALI. (A) Formation of a layer of mucus (arrow) by differentiated S-ALI after air-lifted for 28 days. (B) Alcian Blue staining of mucin produced by cells. Scale bar = 200 μ m. (C) Tight-junction protein (E-cadherin) expression (arrow) in S-ALI cells. Scale bar = 20 μ m. (D) Persistent transepithelial electrical resistance (TEER) across the monolayer of S-ALI. n = 4 biological replicates. (E) Transmission electron micrograph of an S-ALI cell at low magnification. Scale bar = 1 μ m. (F) Under higher magnification, formation of cilia was observed in S-ALI (arrow). Scale bar = 0.5 μ m. (G) Ultrastructural characteristics of cilia (arrow) on S-ALI. Each cilium is anchored to the apical membrane of the cell. Scale bar = 0.2 μ m. (H) Membrane surface of undifferentiated SAECS. Scale bar = 0.2 μ m.

Lung Epithelial Progenitors Injury and Epithelial plasticity

- ✓ PM2.5 disrupted AT2-to-AT1 differentiation by altering signaling pathways, including MAPK signaling, Wnt signaling, and pathways regulating the pluripotency of stem cells.

Yu H et al. Respiratory Research 2022

- ✓ DEP impaired lung organoid development and downregulated WNT/ β -catenin signaling which is essential to promote epithelial repair.

Wu X et al. Environ Pollution 2022

- ✓ PM exposure decreases ciliated and club cells. Also goblet cells expansion observed. These suggests epithelial plasticity*

*Epithelial plasticity: ability of epithelial cells to reversibly change phenotype

Kayalar O et al. Frontiers in Immunology 2024 [REVIEW]

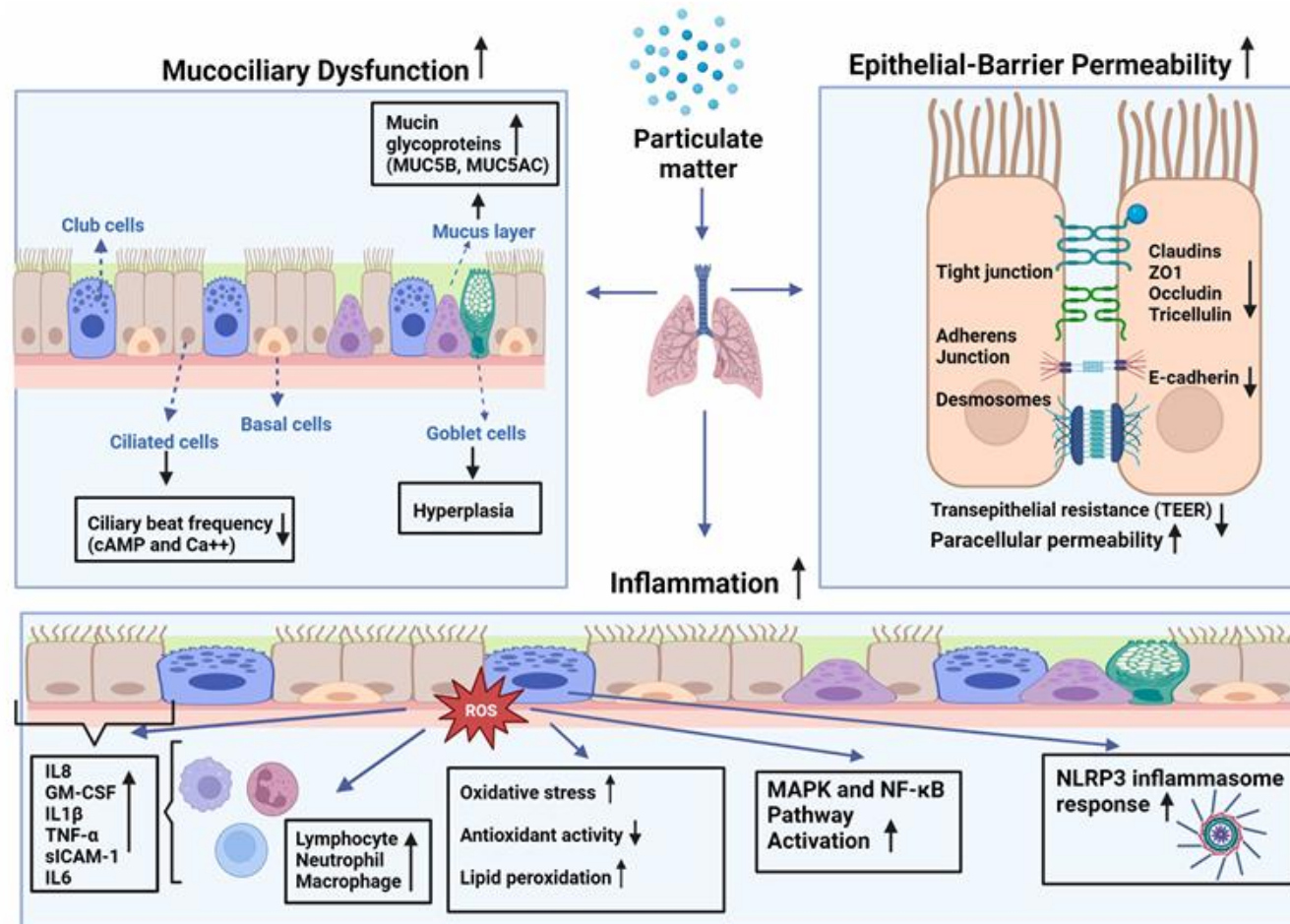


FIGURE 1

Effects of particulate matter (PM) on mucociliary function, epithelial barrier integrity, and inflammatory changes in airways: PM leads to increased production of reactive oxygen species (ROS) leading to higher oxidative stress in the cell, as well as lipid peroxidation and diminished antioxidant capacity. This imbalance causes augmented expression of inflammatory mediators such as interleukin (IL)-1 β , -6, -8, tumor necrosis factor (TNF)- α , granulocyte macrophage-colony stimulating factor (GM-CSF), and soluble intercellular adhesion molecule (sICAM)-1 by epithelial cells and inflammatory cells such as macrophages, neutrophils, and lymphocytes at the site of the inflammation. Increased inflammation may attract more inflammatory cells and lead to increased cytokine production that may cause activation of mitogen-activated protein kinase (MAPK), and nuclear factor-kappa B (NF- κ B) pathways, and nod-like receptor pyrin domain-containing 3 (NLRP3) inflammasome response.

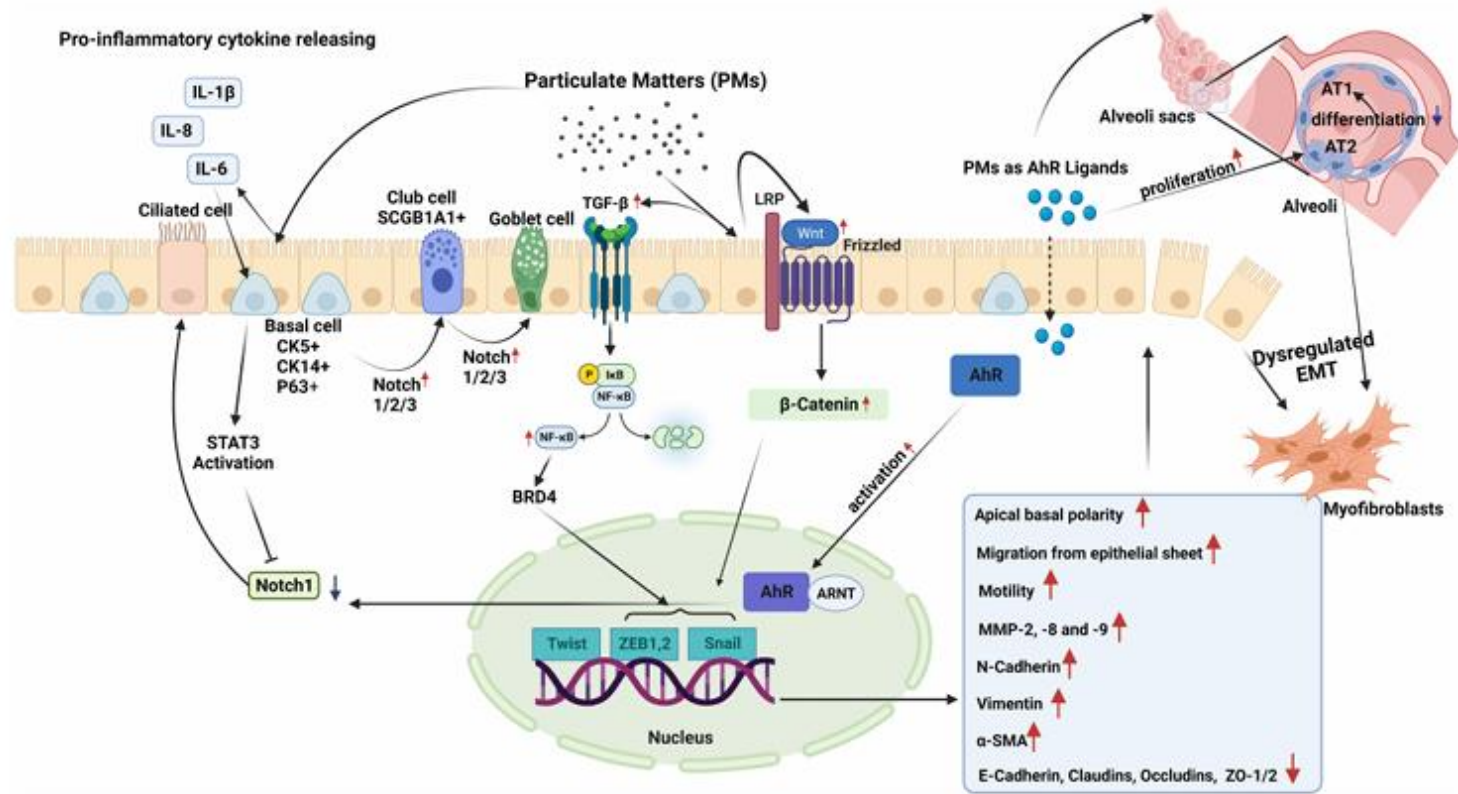
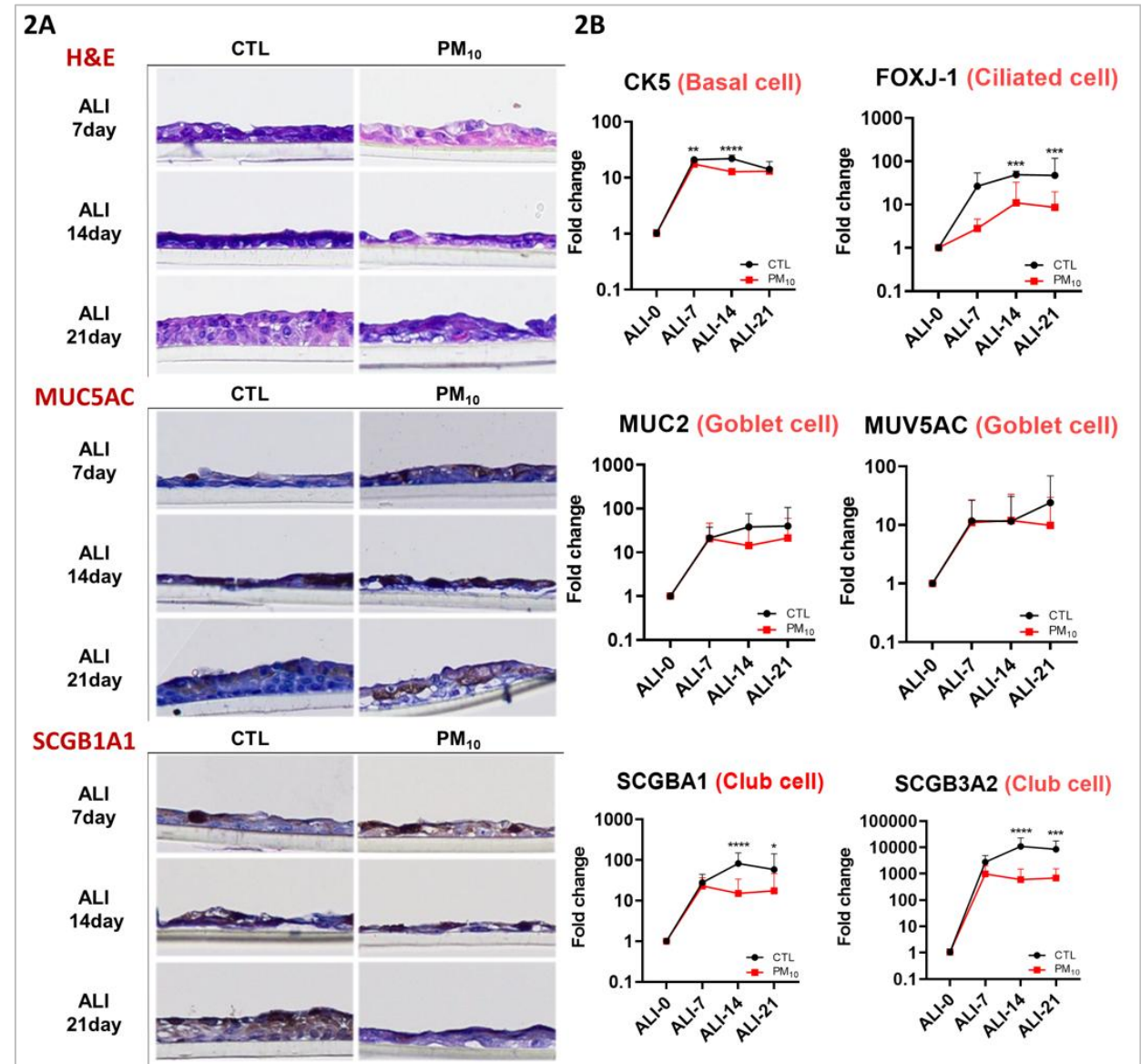
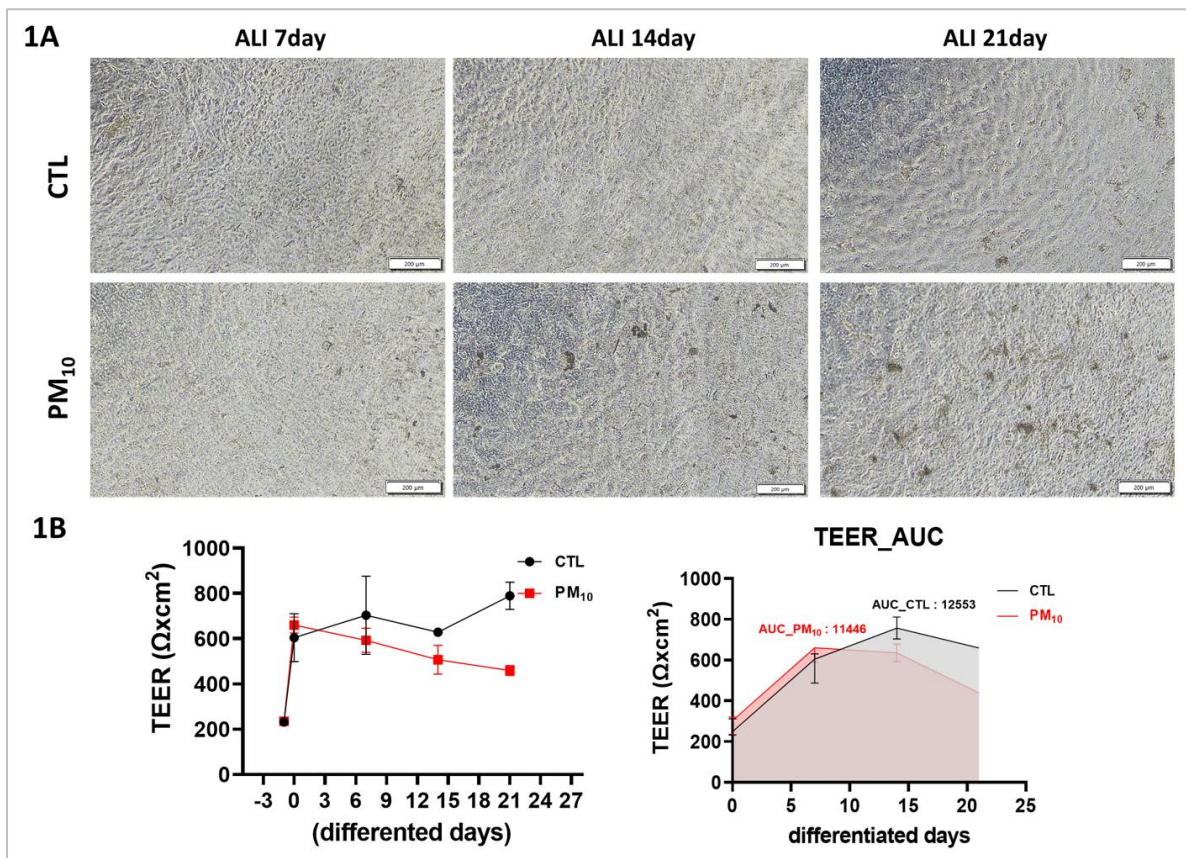
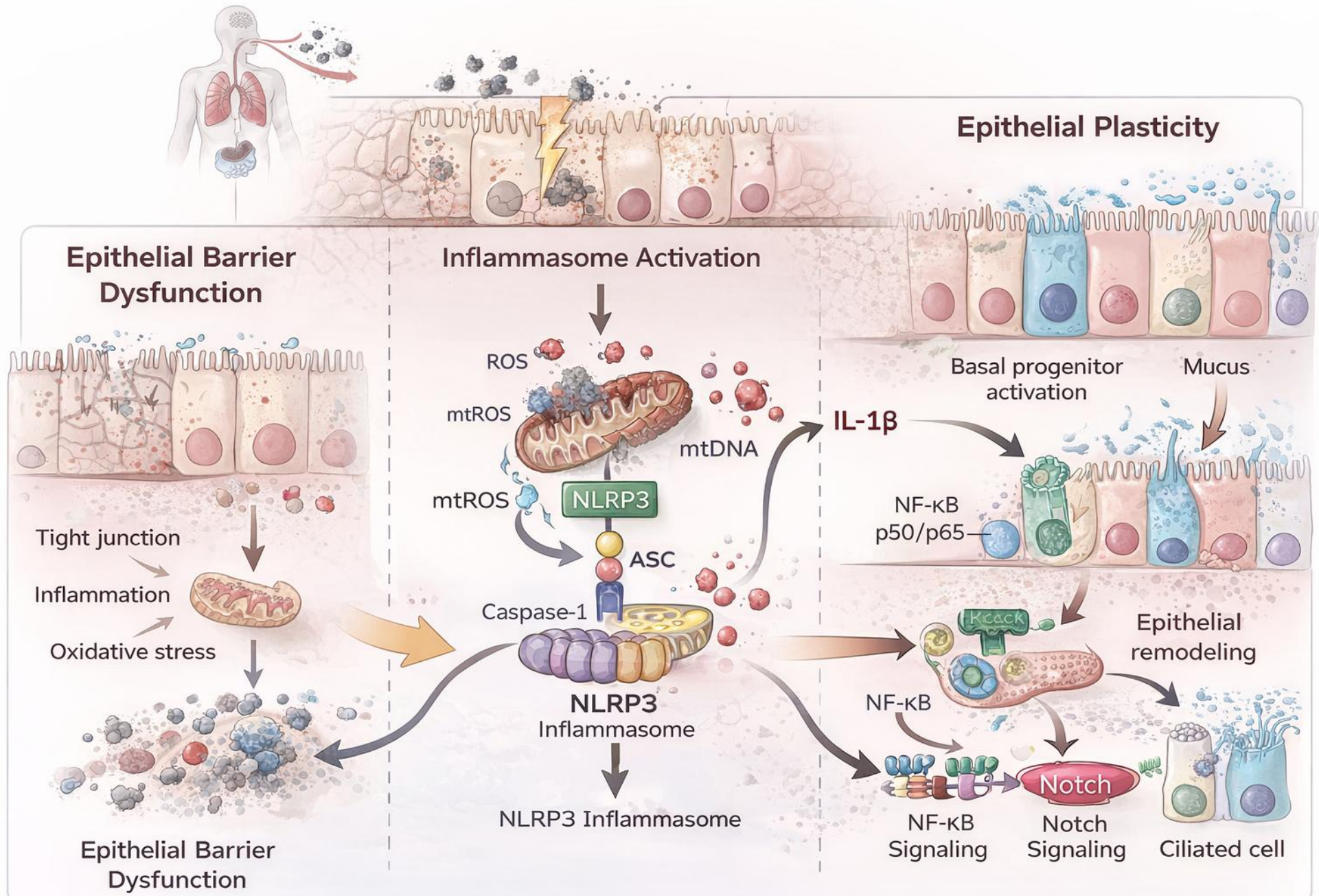


FIGURE 2

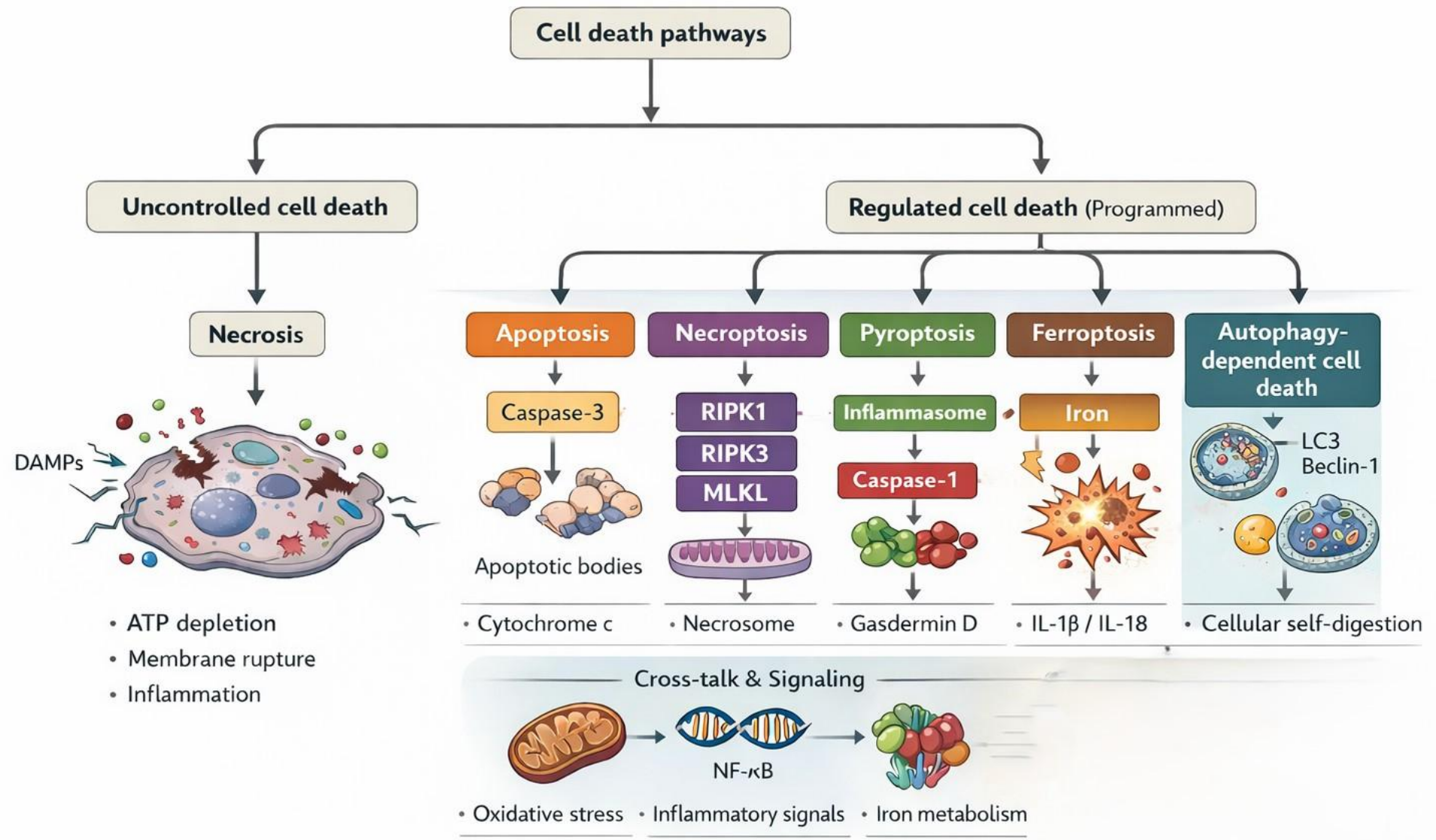
Epithelial plasticity and impact of particulate matter (PM): Exposure to PM in short term, leads to inhibition of Notch1 by stimulating STAT3 and aryl hydrocarbon receptor (AhR) activation in basal epithelial cells. Decreased Notch1 activation leads to differentiation of progenitor/stem cells into ciliated cells. Conversely, longer PM exposure results in increased expression and activation of Notch1/2/3, which induce basal progenitor cells to differentiate into secretory and mucus-producing cells. In areas where there are fewer basal cells, Notch activation stimulates SCG1A1+ club cells to differentiate to goblet cells. Smaller PM ($\leq 2.5\mu\text{M}$) reaching the alveoli stimulates the proliferation of alveolar type (AT) 2 cells, and induces the differentiation of these cells to myofibroblasts, while preventing their differentiation into AT1 cells. In case of chronic exposure, PM activates the TGF- β -NF κ B and Wnt/ β -catenin pathways. These pathways activate the Twist, Snail, and Zeb transcription factor module, initiating a process called dysregulated epithelial-mesenchymal transition (EMT). During EMT, there are noticeable changes in apical-basal polarity, migration of epithelial cells from the epithelial sheet, increases in the expression of MMP-2, 8, and 9. E-cadherin, occludin, claudin and zonula occludens-1 show a decreasing pattern of change, while mesenchymal cell markers such as N-cadherin, Vimentin, and α -SMA increase.





Schematic illustration of epithelial plasticity created by the author.

Cell Death Pathways



Schematic illustration of cell death pathways created by the author.

PM-Inflammasome

- ✓ NLRP3 inflammasome activation by PM in macrophages, lung epithelial cells

Caceres L et al. Environmental Pollution 2024

Lee C et al. Molecular Immunology 2019

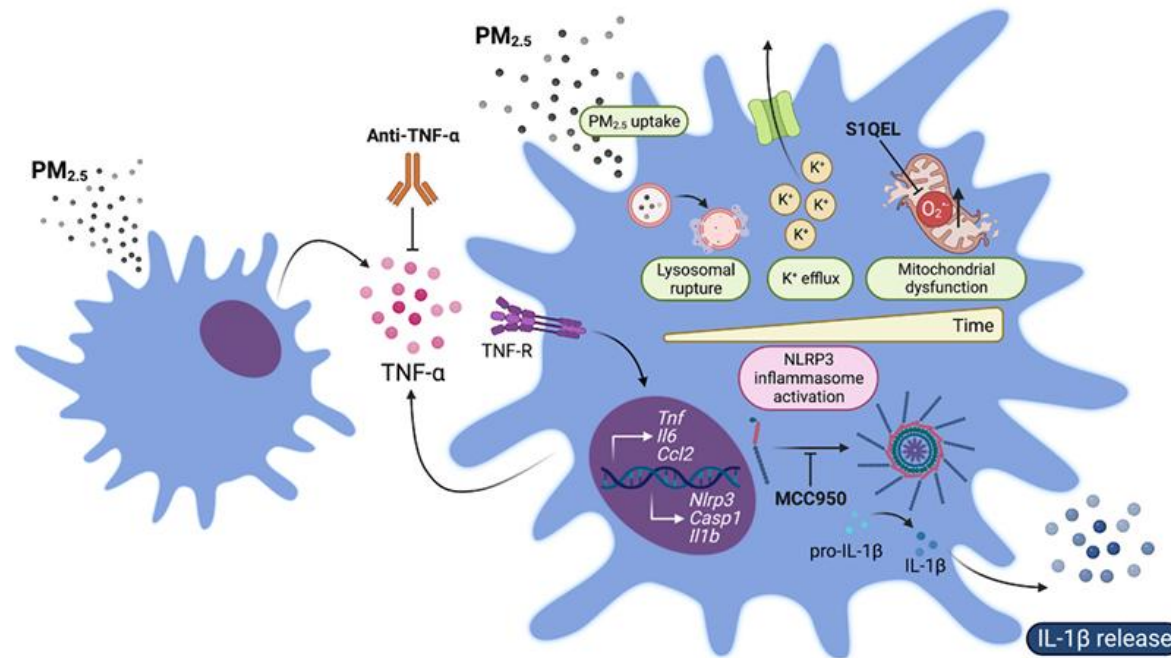


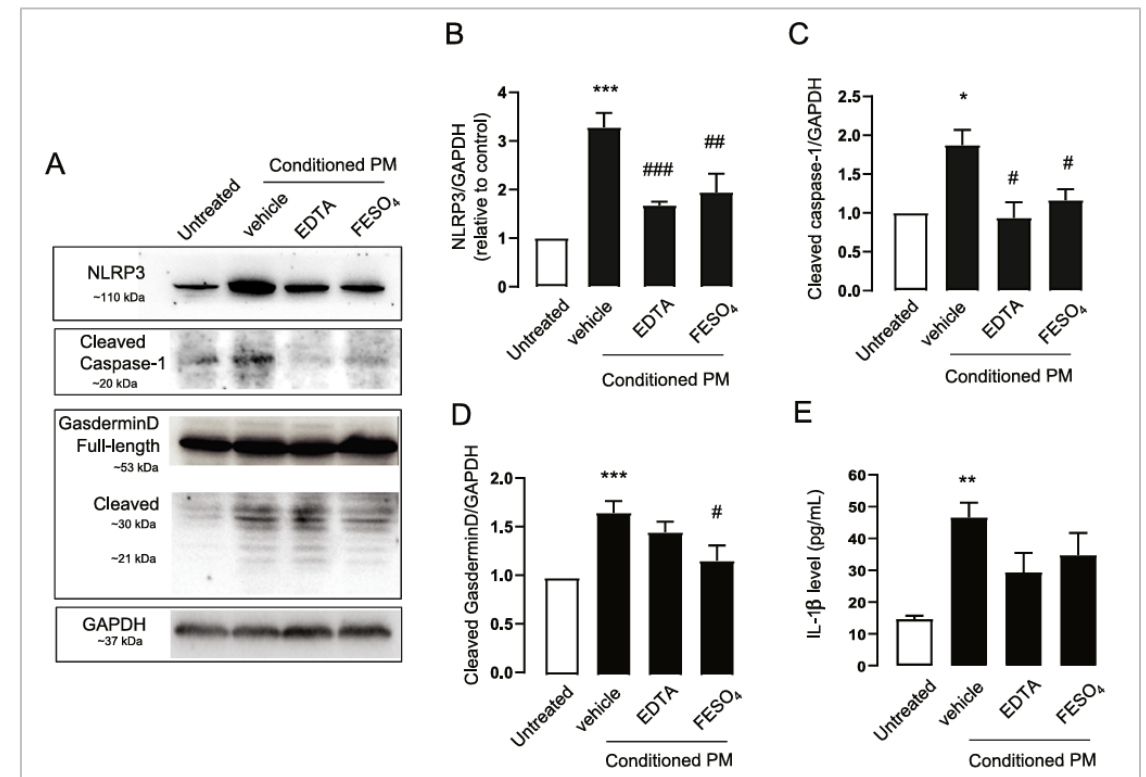
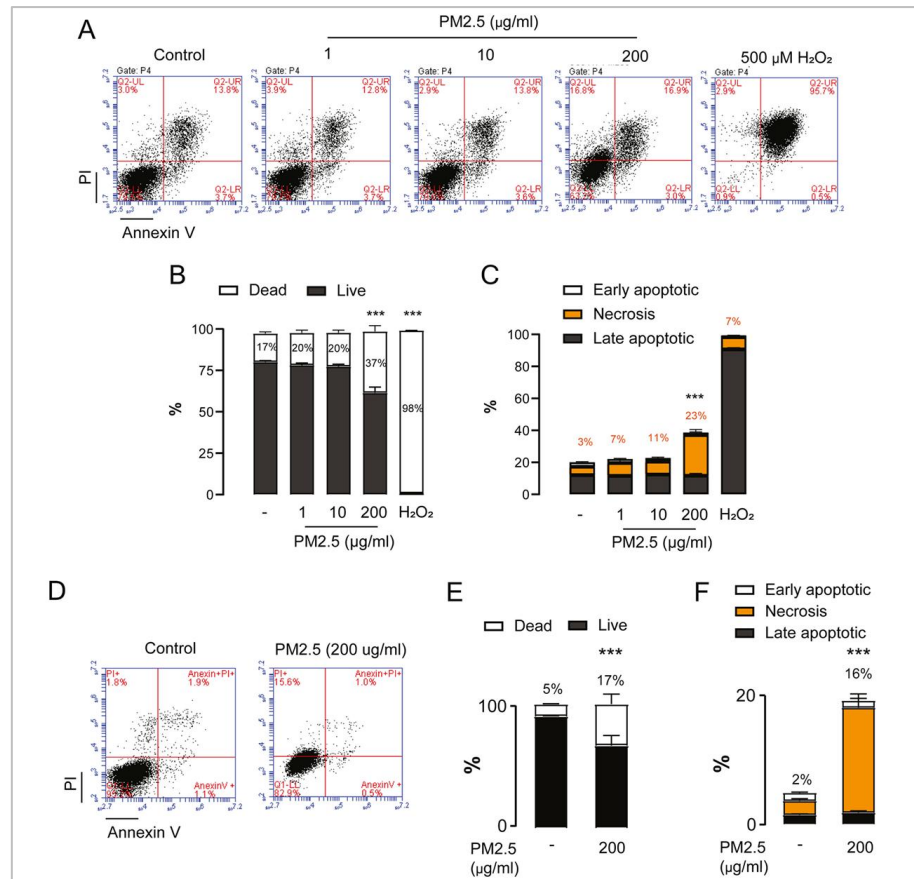
Fig. 6. Mechanistic insights into NLRP3 inflammasome activation and IL-1 β release by PM_{2.5}. PM_{2.5} uptake by macrophages promotes gene expression of pro-inflammatory cytokines and inflammasome priming (i.e. upregulation of *Nlrp3*, *Casp1*, and *Il1b*). Lysosomal rupture, K⁺ efflux, and O₂^{•-} production from mitochondrial Complex I sequentially promote NLRP3 inflammasome oligomerization, ASC-specks formation, pro-IL-1 β cleavage by activated Caspase-1, and IL-1 β release. PM_{2.5}-induced inflammation involves cytokine production, such as of TNF- α , which further contributes to NLRP3 inflammasome activation and IL-1 β production. TNF- α blockade, O₂^{•-} scavenging by S1QEL 1.1, and inhibition of NLRP3 oligomerization by MCC950 reduces PM_{2.5}-induced IL-1 β release in macrophages.

Inflammasome-mediated pyroptosis

- ✓ PM2.5 and chromium(VI)-induced acute cytotoxicity in human airway epithelial cells via inflammasome-mediated pyroptosis*

*Pyroptosis: programmed necrosis that is closely associated with inflammatory signaling through the activation of NLRP3 inflammasome

Moonwiriyaik A et al. Environmental Toxicology and Pharmacology 2024



Ferroptosis

- ✓ PM2.5 induced ferroptosis* in lung epithelial cells through Nrf2-PPAR-ferritinophagy signaling pathway.

*Ferroptosis: non-apoptotic programmed cell death primarily dependent on intracellular iron overload and lipid peroxidation

Wang Y et al. Free Radical Biology and Medicine 2022

- ✓ There is the link between ferroptosis and inflammasome induced by PM2.5 through iron-ROS axis in macrophages.

Park M et al. Cell Death Discovery 2024

PM-Ferroptosis and Inflammasome

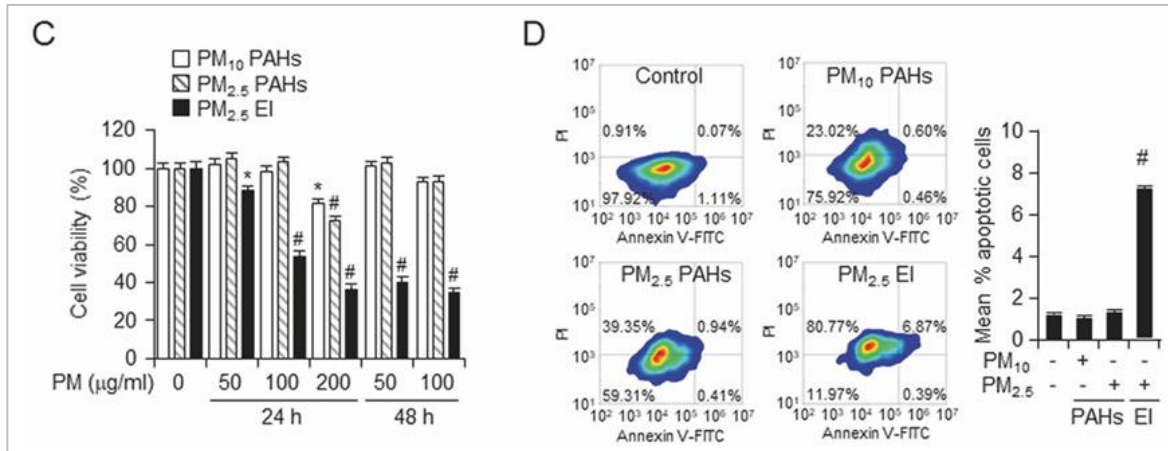


Fig. 1 PM-induced cell deaths in macrophages

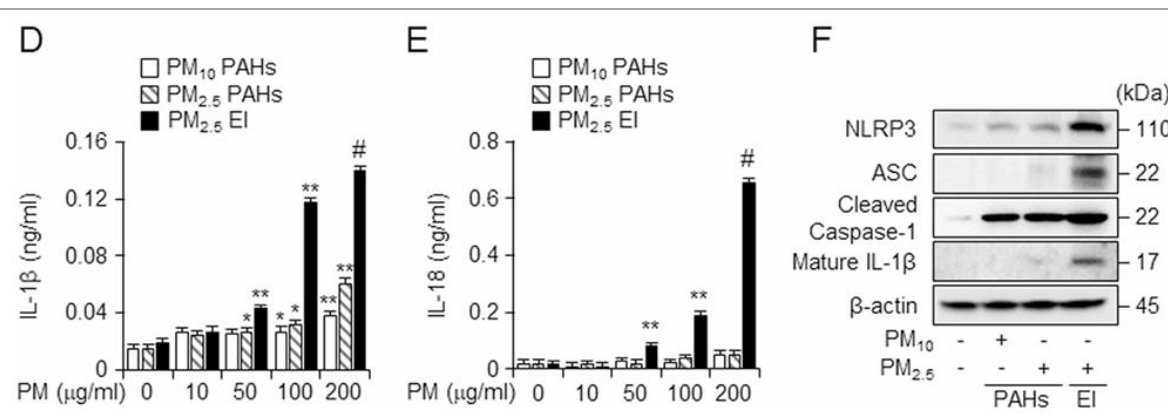


Fig. 2 PM-induced inflammation, inflammasome

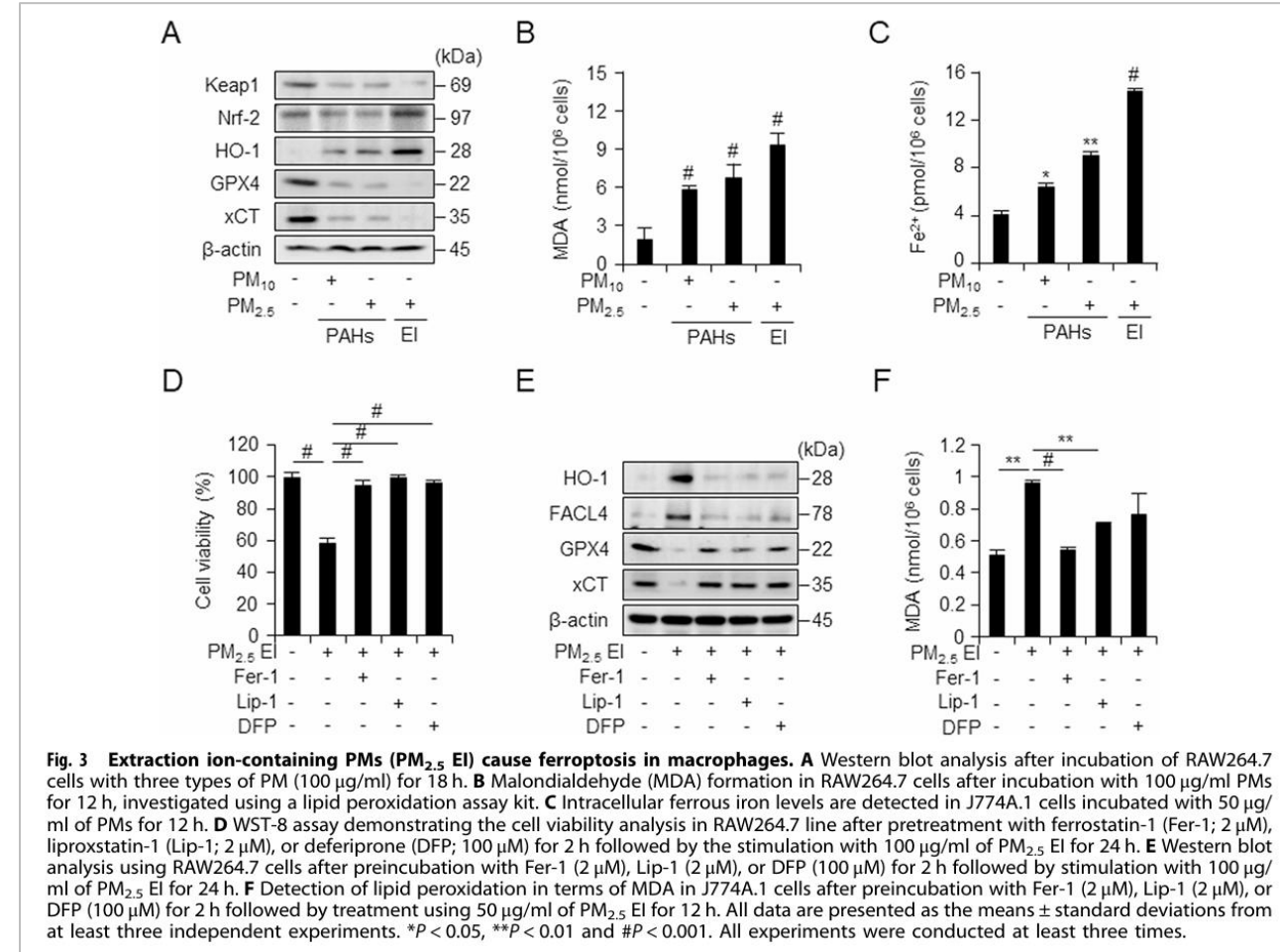


Fig. 3 Extraction ion-containing PMs (PM_{2.5} EI) cause ferroptosis in macrophages. **A** Western blot analysis after incubation of RAW264.7 cells with three types of PM (100 μg/ml) for 18 h. **B** Malondialdehyde (MDA) formation in RAW264.7 cells after incubation with 100 μg/ml PMs for 12 h, investigated using a lipid peroxidation assay kit. **C** Intracellular ferrous iron levels are detected in J774A.1 cells incubated with 50 μg/ml of PMs for 12 h. **D** WST-8 assay demonstrating the cell viability analysis in RAW264.7 line after pretreatment with ferrostatin-1 (Fer-1; 2 μM), liproxstatin-1 (Lip-1; 2 μM), or deferiprone (DFP; 100 μM) for 2 h followed by the stimulation with 100 μg/ml of PM_{2.5} EI for 24 h. **E** Western blot analysis using RAW264.7 cells after preincubation with Fer-1 (2 μM), Lip-1 (2 μM), or DFP (100 μM) for 2 h followed by stimulation with 100 μg/ml of PM_{2.5} EI for 24 h. **F** Detection of lipid peroxidation in terms of MDA in J774A.1 cells after preincubation with Fer-1 (2 μM), Lip-1 (2 μM), or DFP (100 μM) for 2 h followed by treatment using 50 μg/ml of PM_{2.5} EI for 12 h. All data are presented as the means ± standard deviations from at least three independent experiments. **P* < 0.05, ***P* < 0.01 and #*P* < 0.001. All experiments were conducted at least three times.



Future Research Directions

- ✓ Single-cell approach
- ✓ Organoid-based toxicology
- ✓ Spatial transcriptomics
- ✓ Targeting inflammasome pathways
- ✓ Ferroptosis-based therapeutics

